ELSEVIER

www.elsevier.nl/locate/jorganchem

Journal of Organometallic Chemistry 607 (2000) 213–221

Journal of Organometallic Chemistry

Intramolecular N···E interactions in N-functionalised alkyl complexes $R'ECl_2$ (E = P, As, Sb; R = 6-Me-2-Pyr$(SiMe_3)_2C^-$)

Tania R. van den Ancker [a], Philip C. Andrews [b], Simon J. King [b], John E. McGrady [c], Colin L. Raston [b,*], Brett A. Roberts [b], Brian W. Skelton [d], Allan H. White [d]

[a] *Faculty of Sciences, Department of Biological and Physical Sciences, University of Southern Queensland, Toowoomba, Qld 4350, Australia*
[b] *Department of Chemistry, Monash University, Clayton, Melbourne, Vic. 3800, Australia*
[c] *Department of Chemistry, University of York, Heslington, York YO10 5DD, UK*
[d] *Department of Chemistry, University of Western Australia, Nedlands, WA 6907, Australia*

Received 20 May 2000; received in revised form 15 June 2000

Dedicated to Professor Martin A. Bennett on the occasion of his 65th birthday.

Abstract

The metathetical exchange reactions of $R'Li{\cdot}Et_2O$ [R′ = 6-Me-2-Pyr$(SiMe_3)_2C^-$] with ECl_3 (E = P, As, Sb) give the neutral E(III) complexes, $R'ECl_2$. All complexes have been crystallographically characterised and exhibit extremely short intramolecular N···E dative bonds, with the phosphorus derivative exhibiting the shortest neutral N···P dative bond of 2.238(1) Å. Theoretical studies performed with approximate density functional theory successfully model the unusual structural features of compound $R'PCl_2$, although the magnitude of the effect is somewhat underestimated. Under the same conditions, the lithium complex of the less bulky ligand r′ [r′ = 6-Me-2-Pyr$(SiMe_3)CH^-$] affords a weakly associated, dimeric complex $[r'SbCl_2]_2$, (via Sb–Cl···Sb bridging) which is a consequence of less steric compression from the alkyl group around the metal centre; intramolecular N···Sb coordination is also present.

Keywords: Intramolecular; Dative bonding; Group 15; Alkyl halides

1. Introduction

The use of bulky alkyl or aryl groups has become common practice in the stabilisation, or attempted stabilisation, of double bonded species (E=E) of the heavier Group 15 elements [1]. Examples include 2,4,6-tri-*tert*-butylphenyl [2], used in the synthesis of $[P(C_6H_2)(^tBu)_3\text{-}2,4,6]_2$ and 2,4,6-tris(bis(trimethylsilyl)-methyl)phenyl [3], used in the synthesis of $[Bi(C_6H_2\text{-}\{CH_2(SiMe_3)_2\}_3\text{-}2,4,6)]_2$. Some of the most extensively studied ligands are those which contain one or more trimethylsilyl groups. Previously, we have reported [4] some main group chemistry of the bis-silylated ligands 2-Pyr$(SiMe_3)_2C^-$ (R) and 6-Me-2-Pyr$(SiMe_3)_2C^-$ (R′), which exhibit various types of bonding, e.g. η^1-alkyls $[(LiR)_2]$, ionic species $[AlR_2]^+[AlCl_4]^-$, head to tail coupled dialkyls, [2-Pyr$(SiMe_3)_2$CH-R] [4], chelated species [5] and [2 + 2] cycloaddition derivatives [6]. As well as the steric bulk offered by the two trimethylsilyl groups, both R and R′ are devoid of β-hydrogens negating the possibility of decomposition via β-hydride elimination although, their complexes can undergo elimination of Me_3SiCl to give the corresponding metal–metalloid alkene type species [6]. There is also the possibility of additional stabilisation through intramolecular coordination to the metal–metalloid centre resulting from internal lone pair electron donation from the pyridyl nitrogen.

The common synthetic pathway in the synthesis of many multiple bonded species involves the formation of the alkyl–aryl dihalide precursor, followed by subsequent reduction with a variety of metals–metal reagents [7]. In assessing the ability of R′ to stabilise

* Corresponding author. Fax: +61-3-99054597.
E-mail address: c.raston@sci.monash.edu.au (C.L. Raston).

0022-328X/00/$ - see front matter
PII: S0022-328X(00)00374-0

E=E bonds we have synthesised and characterised the intermediate complexes, R′ECl_2 (E = P, As, Sb; **1**–**3**). Single crystal X-ray structure determinations show that these complexes exhibit rare and short intramolecular N···E dative bonds. For comparison with **3** we also report the synthesis and structure of [r′$SbCl_2$]$_2$ (**4**), the corresponding antimony complex with the alkyl group bearing only one trimethylsilyl substituent, which assists in elucidating any effect of steric hindrance on intramolecular N···E coordination and association, at least for antimony.

2. Results and discussion

2.1. Synthesis and characterisation

In a typical reaction, Scheme 1, R′H was metallated with ^{n}BuLi in Et_2O at 0° and the mixture cooled to −78°C where it was added slowly to a −78°C Et_2O solution of ECl_3 (E = P, As, Sb). The resulting suspension was stirred and allowed to warm slowly to ambient temperature over 6 h. Filtration and extraction into hexane followed by in vacuo concentration of the solution and cooling to −30°C resulted in modest yields of **1** (66%), **2** (68%) and **3** (74%). Compound **4** was prepared under the same conditions in THF and extracted into hexane after filtration. Concentration and cooling to −30°C resulted in the crystallisation of **4** in a 58% yield.

Compound **1** crystallises as large orange plates. When isolated as a solid, **1** exhibits low thermal stability, decomposing over several hours at 25°C, presumably through Me_3SiCl elimination to give an unstable P=C intermediate. Compound **2** crystallises as yellow cuboids, which when isolated as a solid and stored under argon exhibit a greater degree of thermal stability than **1**, being stable at 25°C over several weeks.

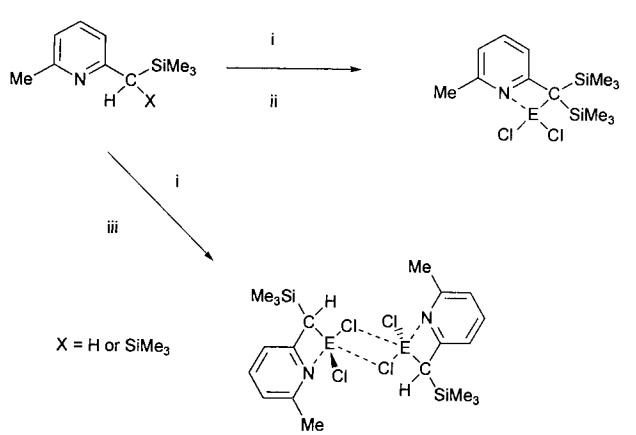

Scheme 1. Reagents and conditions: (i) ^{n}BuLi, Et_2O or THF, 0°C; (ii) ECl_3, Et_2O, −78°C, 6 h, E = P, As, Sb; (iii) $SbCl_3$, THF, −78°C, 6 h.

Compound **3** crystallises as colourless prisms in the triclinic space group $P\bar{1}$ with one molecule in the asymmetric unit. It is thermally stable at ambient temperature, remaining intact up to its melting point of 127°C. Compound **4** crystallises as colourless prisms. It exhibits lower thermal stability than its bis-silylated analogue, decomposing over several days when stored under argon at room temperature. Group 15 chemistry has been thwarted by decomposition/competing reactions. In a previous study on the slightly less bulky RECl_2 [5] complexes it was found that the antimony complex was the most stable, the arsenic compound decomposing rapidly at 78°C and slowly at 20°C with elimination of Me_3SiCl. Facile elimination in the analogous phosphorus complex also occurs at > −10°C, resulting in the formation of a red–brown oil. The extra bulk offered by the methyl group in the 6 position on the pyridine ring results in the analogous dihalide complexes exhibiting much greater thermal stability.

Mild thermolysis of R$SbCl_2$ results in the elimination of Me_3SiCl to give the chloro-bridged polymeric geminal C-centred distibine complex [2-Pyr($SiMe_3$)CSbCl]$_\infty$ [6]. This complex contains an almost square, but buckled C_2Sb_2 core with an internally bridged Cl linking the two metal centres. As a result of such crowding, the N···Sb distances are shortened to 2.220(8) Å. Thermolysis of R′$SbCl_2$ in toluene under the same condition results in the elimination of Me_3SiCl to yield an oil, presumably of polymeric nature.

2.2. X-ray structure determination

The results of the structural studies of **1**–**4** are consistent, in respect of stoichiometry, connectivity and stereochemistry, with their formulation as species of the type R′ECl_2 (E = P, As, Sb, **1**–**3**) or r′$SbCl_2$, **4**; Complexes **1**–**3** exhibit one molecule of complex devoid of any crystallographic symmetry comprising the asymmetric unit of the structure, with complex **4** being a loosely associated centrosymmetric dimer. Comparative geometries, given in Table 1, show that despite the weak association found in **4**, there is a remarkable similarity across all four compounds, after due regard for the different metal atom radii. Fig. 1(a) depicts **2** as a representative of **1**–**3**, with the dimer of **4** being given in Fig. 1(b). In all complexes, the E atom is chelated by the pyridyl nitrogen, with C(1) of the ligand forming a four membered ring, which is essentially planar and coplanar in the pyridine ring and Cl(2), with Cl(2)–E–N(12) forming the axis of a distorted trigonal bipyramidal array in which the lone pair is equatorial. The disposition of the $SiMe_3$ moieties is remarkably constant across the arrays, presumably dictated by steric interactions with the other components about the E-centre.

Table 1
Selected molecular geometries, **1**–**4** [a]

Compound (M)	**1** (P)	**2** (As)	**3** (Sb)	**4** (Sb)
Distances (Å)				
M–Cl(1)	2.079(2)	2.189(2)	2.366(2)	2.393(1)
M–Cl(2)	2.203(2)	2.327(1)	2.466(1)	2.494(1)
M–C(1)	1.879(4)	2.022(3)	2.218(3)	2.177(4)
M–N(12)	2.238(1)	2.285(2)	2.391(3)	2.418(3)
C(1)–C(11)	–	1.514(4)	1.501(4)	1.503(5)
C(1)–Si(1)	–	1.931(4)	1.917(4)	1.901(4)
C(1)–Si(2)	–	1.924(4)	1.914(4)	–
N(12)–C(13)	–	1.341(4)	1.340(5)	1.354(5)
C(13)–C(14)	–	1.386(6)	1.384(6)	1.382(6)
C(14)–C(15)	–	1.351(6)	1.374(7)	1.365(8)
C(15)–C(16)	–	1.393(5)	1.370(5)	1.380(6)
C(11)–C(16)	–	1.388(5)	1.391(5)	1.392(6)
C(11)–N(12)	–	1.340(4)	1.349(5)	1.339(6)
Angles (°)				
Cl(1)–M–Cl(2)	92.83(7)	92.57(5)	91.47(5)	91.90(5)
Cl(1)–M–C(1)	108.6(1)	106.7(1)	102.9(1)	99.6(1)
Cl(2)–M–C(1)	97.4(1)	97.73(8)	96.39(9)	95.0(1)
Cl(1)–M–N(12)	–	89.85(9)	85.84(9)	88.73(8)
Cl(2)–M–N(12)	–	163.33(8)	156.36(8)	155.55(9)
C(1)–M–N(12)	–	65.8(1)	61.6(1)	60.9(1)
M–C(1)–Si(1)	–	117.1(2)	117.3(2)	123.2(2)
M–C(1)–Si(2)	–	107.1(2)	107.6(1)	–
M–C(1)–C(11)	95.6(2)	94.0(2)	94.0(2)	95.5(3)
C(11)–C(1)–Si(1)	–	107.8(2)	107.4(2)	111.3(2)
C(11)–C(1)–Si(2)	–	113.4(2)	114.8(2)	–
Si(1)–C(1)–Si(2)	–	115.6(2)	114.3(2)	–
M–N(12)–C(11)	86.0(2)	88.0(2)	90.9(2)	89.9(2)
M–N(12)–C(13)	–	148.6(2)	146.6(3)	146.0(3)
C(1)–C(11)–N(12)	108.4(3)	110.8(3)	112.0(3)	110.5(3)
C(1)–C(11)–C(16)	–	129.0(3)	127.9(3)	128.6(4)
N(12)–C(13)–C(131)	–	116.9(3)	117.2(4)	116.5(4)
C(14)–C(13)–C(131)	–	124.4(3)	123.3(4)	124.7(4)
N(12)–C(11)–C(16)	–	120.2(3)	120.0(3)	120.9(3)
C(11)–N(12)–C(13)	–	122.5(3)	122.0(3)	121.8(3)
N(12)–C(13)–C(14)	119.7(3)	118.7(3)	119.5(4)	118.8(4)
C(13)–C(14)–C(15)	–	120.3(3)	119.2(4)	119.9(4)
C(14)–C(15)–C(16)	–	120.6(4)	121.0(4)	121.1(4)
C(11)–C(16)–C(15)	–	117.7(4)	118.3(4)	117.4(5)
Torsion angles (°)				
C(11)–N(12)–M–Cl(1)	–	116.4(2)	115.1(2)	113.4(2)
C(11)–N(12)–M–C(1)	–	8.0(2)	8.1(3)	11.7(2)
Cl(1)–M–C(1)–Si(1)	–	23.2(2)	26.7(2)	26.4(2)
Cl(1)–M–C(1)–Si(2)	–	154.9(1)	157.2(1)	–
Cl(1)–M–C(1)–C(11)	–	−89.2(2)	−85.3(2)	−93.6(2)
M–C(1)–Si(1)–C(111)	–	−49.3(3)	46.8(3)	51.0(3)
M–C(1)–Si(1)–C(112)	–	169.3(2)	168.9(2)	169.8(2)
C(11)–C(1)–Si(1)–C(113)	–	30.3(3)	29.6(3)	39.1(4)
M–C(1)–Si(2)–C(213)	–	26.1(2)	27.3(3)	–
M–C(1)–Si(2)–C(212)	–	−95.5(2)	−91.8(2)	–
C(11)–C(1)–Si(2)–C(211)	–	41.4(3)	42.6(4)	–
Deviations from the NC_5 aromatic plane, δ (Å)				
δM	–	0.330(5)	0.273(6)	0.552(6)
δC(1)	–	−0.057(6)	−0.130(6)	−0.081(7)
δSi(1)	–	−1.816(6)	−1.896(6)	−1.759(7)
δSi(2)	–	1.415(6)	1.269(7)	–

[a] In **4**, Sb–Cl(2) ($\bar{x}$, $\bar{y}$, $\bar{z}$) is 3.352(1) Å; Sb···Sb, Cl···Cl being 4.2450(8), 3.763(2) Å. Sb–Cl(2)–Sb is 101.38(5) and Cl(2)–Sb–Cl(2) 78.62(4)°.

The most important and unusual feature of **1** is the remarkably short nitrogen to phosphorus bond distance of 2.238(1) Å, which to our knowledge is the shortest known N···P dative bond established for a neutral P(III) complex [8].

The dative bond between the N and the P forms part of the four membered chelate ring N(1)–P(1)–C(1)–C(2) which is co-planar in the pyridine ring. The bond distance of 2.238(1) Å is short with comparison to those reported [9] in the structures of tris(8-dimethylamino-1-napthyl)phosphane and tris[2-(dimethylaminomethyl)-phenyl]phosph-ane which also show weak N···P interactions on a neutral phosphorus centre, but with much longer average bond lengths of 2.83 and 3.03 Å.

In contrast, a shorter N–P interaction is found in 2,6-bis[{(dimethylamino)methyl} phenyl]phosphorus-hexafluorophosphate, $[R_2P]^+[PF_6]^-$, [10] a complex exhibiting a formal phosphorus containing cation; in the cation, both amine 'arms' are coordinated to the phosphorus centre to give a pseudo five coordinate phosphorus with short N···P bond distances of 2.082(3) and 2.068(4) Å. Given the electropositive nature of the P centre, it is not unexpected that these bonds are extremely short. Although the neutral, four coordinate $R'PCl_2$ complex does contain a δ^+ phosphorus, charges on the two complexes differ significantly and a true comparison of the N···P interaction cannot be made.

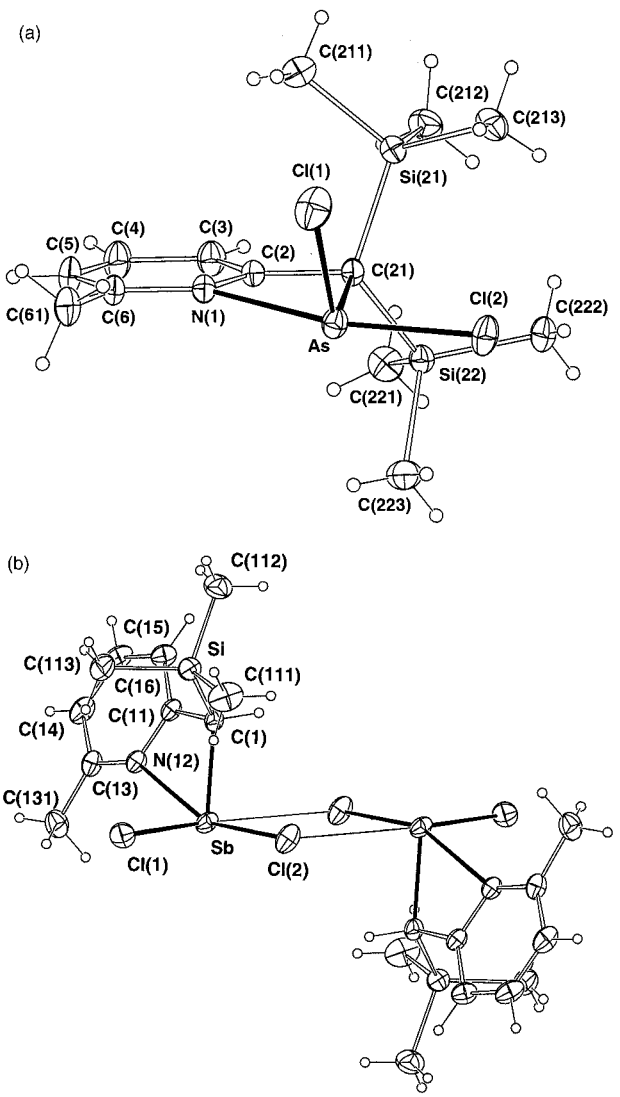

Fig. 1. (a) Molecular structure of $R'AsCl_2$ (**2**), as representation of **1**–**3**. 20% thermal ellipsoids are shown for the non-hydrogen atoms, hydrogen atoms arbitary radii of 0.1 Å. (b) Molecular structure of $[r'SbCl_2]_2$ (**4**), showing its binuclear nature.

The N···P dative bond distance seen in **1**, is much longer than that established for formal covalent N–P bonds, as exemplified by tetrachloro-(*N*,*N*′-dimethylbenzamidino-*N*,*N*′)-phosphorus(V) [11] and [{2-(methylamino)pyridinato}tetrachlorophosphorus(V)] [12], which have N–P bond lengths of 1.810(2) and 1.807(2) Å and 1.845(4) and 1.763(4) Å, respectively. On the other hand, the dative bond in **1** is notably shorter than the sum of the van der Waals radii of nitrogen and phosphorus, 3.4 Å [13].

The P–C bond distance 1.879(4) Å is unremarkable being similar to that found in dichloro (pentabenzyl–cyclopentadienyl)phosphine, 1.866(2) Å [14]. The average P–Cl bond length of 2.14(2) Å, is slightly longer than the mean P–Cl bond lengths in pyrazine–phosphorus(V) pentachloride, 2.09 Å [15] or in dichloro-(pentabenzyl–cyclopentadienyl) phosphine 2.081(1) Å [14].

As with **1**, there is evidence in compound **2** of a short N···E dative bond, with a N···As bond distance of 2.285(2) Å. In reviewing the literature, great variation is found in the reported N···As bond lengths [16–18]. The dative bond in **2**, 2.285(2) Å, which is at the shorter end of the range, is comparable to the N–As bond in Me_3N–$AsCl_3$ [16], 2.286(23) Å, and [{8-(Me_2N)-$C_{10}H_6$}$AsCl_2$], 2.351(9) Å [17], but notably much shorter than those found in [*tert*-butyl{chloro-(2,2,6,6 - tetramethylpiperidine)boryl}amino - arsenicdichloride] [18], 2.619 Å, and in [tris-{2-(Me_2NCH_2)-C_6H_4As}] [19], 2.936(5), 2.961(5) and 3.030(6) Å, which exhibit weak secondary interactions between pendant amines and the arsenic centre.

As expected, formal N–As covalent bonds are much shorter than the dative bond found in **2**. This is evident in the N–As bond lengths in 2,4-dichloro-1,3-bis[2,4,6-tris(trifluoromethyl)phenyl] - 1,3,2λ^3,4λ^3 - diazadiarsetidine, 1.865(3) and 1.852(3) Å [20], and in $(C_6H_4ONH)_2AsPh$ [21], 1.806(3) and 1.807(3) Å. The dative bond, however, is much less than the sum of the van der Waals radii for arsenic and nitrogen, 3.5 Å [19].

There is nothing exceptional in the Cl(1)–As–Cl(2) bond angle of 92.57(5)° which is comparable to that of 93.5(4)° in NMe_3AsCl_3 [16], but closer to right angles when compared with 98.7(1)° in [*tert*-butyl{chloro-(2,2,6,6 - tetramethylpiperidine)boryl}amino - arsenic di-

Table 2
Comparison of E–C bond length and N–C–C–E angles between complexes **1**–**3** and R'_2Hg

Compounds	E–C (Å)	a (°)	b (°)	c (°)
$R'PCl_2$ (**1**)	1.879(4)	86.0(2)	108.4(3)	95.6(2)
$R'AsCl_2$ (**2**)	2.022(3)	88.0(2)	110.8(3)	94.0(2)
$R'SbCl_2$ (**3**)	2.218(3)	90.9(2)	112.0(3)	94.0(2)
R'_2Hg	2.15(6)	–	117.9	103.9

chloride] [18] and the remaining Cl–As–Cl in NMe_3-$AsCl_3$ 98.6(4)°.

The intramolecular Sb···N dative bond, 2.39(1) Å, found in **3** is longer than that of the analogous $RSbCl_2$ complex, 2.317(7) Å [5]. Compound **3** has a short Sb···N bond distance by comparison with that found in the tridentate species $[2,6\text{-}(Me_2NCH_2)_2C_6H_3]SbCl_2$ of 2.491(9) and 2.422(8) Å [22], which contains a similar planar chelate ring, consistent with internal solvation by the amine groups. A variety of base coordinated Group 15 aryl halides have been reported [17] which exhibit elongated Sb···N distances compared to those in **3**. Interestingly, the report on the synthesis and structure of $[2\text{-}(Me_2NCH_2)C_6H_4]_2SbCl$ shows that the two amine groups differ in the extent to which they interact with the Sb centre, N(1) being strongly coordinated, Sb(1)–N(1) 2.463(2) Å, and N(2) having only a weak interaction, Sb(1)–N(2) 3.216(3) Å. The orientation of the interaction of N(1) and its substituents is such that the formal lone pair of the NMe_2 is directed toward the Sb centre resulting in a N(1)–Sb–Cl(1) bond angle of 165.58(6)°. Complex **3** behaves in a similar manner, with the lone pair on the N in the pyridine ring being directed towards the Sb metal centre to give a N(1)–Sb–Cl(2) angle of 156.36(8)°.

The two chlorines in **3** are almost set at right angles, Cl(1)–Sb–Cl(2) 91.47(5)°, which is in dramatic contrast to the angle of Cl(1)–Sb–Cl(2), 174.0(1)°, evident in the five-coordinate, less hindered $[2,6\text{-}(Me_2NCH_2)_2C_6H_3]$-$SbCl_2$ complex, which consequently has N(1)–Sb–Cl(2) and N(2)–Sb–Cl(2) angles near right angles 85.3(2) and 94.1(2)°, compared to the near linear arrangement seen in **3**. The structure of a complex with a slightly bulkier hydrocarbyl group, $[8\text{-}(Me_2N)C_{10}H_6]_2SbCl$ [17], exhibits varying interactions with the amine arms having Sb–N bond lengths of 2.519(4) and 2.903(4) Å; both these distances are much longer than in **3**, which is indicative of coordinated and weakly associated interactions.

Formal Sb–N bonds are, as expected, much shorter than the 2.39(1) Å seen in **3**. The Sb(V) complex, $[Ph_3Sb(NCO)_2]$ [23], has a bond length of 2.123(4) Å in which the N–Sb bond distance is close to the sum of single bond covalent radii. Shorter N–Sb bonds are also evident in the chelated complex $[\{Cp'(CO)_2Mn\}_2Sb$-$(dipy)]^+[\{Cp'(CO)_2Mn\}_2SbCl_2]^-$ [24] of 2.266(7) and 2.269(7) and in the five coordinate, highly delocalised structure of $[\{PhC(NSiMe_3)_2\}_2]SbCl$ [25], of 2.169(3), 2.331(3), 2.292(3) and 2.248(3) Å. A true comparison, however, to $R'SbCl_2$ is not possible as there are no formal C–Sb bonds in these complexes.

While the N···Sb distance in **3** is short there is a slight elongation in the Sb–C distance of 2.218(3) Å, perhaps a consequence of steric strain associated with the four membered ring and/or the hybridisation of the C-centre, i.e. sp^3 versus sp^2. Complexes $[2\text{-}(Me_2NCH_2)$-$C_6H_4]_2SbCl$, $[8\text{-}(Me_2N)C_{10}H_6]_2SbCl$ [17] and $[2,6$-$(Me_2NCH_2)_2C_6H_3]SbCl_2$ [22] all have longer N···Sb interactions compared with **3** and exhibit shorter Sb–C bonds of 2.152(3) and 2.160(3), 2.167(5) and 2.164(4) and 2.100(9) Å, respectively, these long bonds diminishing steric crowding. Similarly, the analogous Sb–C distance in $RSbCl_2$, 2.213(5) Å, is elongated [5].

The effect of using the less bulky ligand r′, which contains only one silyl group, is evident in Fig. 1(b). The reduction in steric bulk results in less protection at the antimony centre, and aggregation occurs. Complex **4** is found to be dimeric and not monomeric. As with the $R'SbCl_2$ analogue, a N···Sb interaction is evident, but with a marginally longer bond length of 2.418(3) Å, most likely due to the slightly diminished steric crowding around the Sb and weak halide bridging. The Sb–C bond length of 2.177(4) is marginally shorter than 2.218(3) Å in **3**. Both Sb–Cl bond lengths 2.494(1) and 2.393(1) Å are comparable to the Sb–Cl bond lengths in **3** of 2.466(1) and 2.366(2) Å. In comparison, the bridging Sb–Cl contact is much longer, 3.352(1) Å, and the complex can be regarded as weakly associated, there being little difference between the Cl(1)–Sb(1)–Cl(2) bond angles in **3** and **4** of 91.47(5)°and 91.90(5)°, respectively. Intramolecular complexation of the pyridine nitrogen in **3** and **4** is consistent with the ability of antimony(III) complexes to form adducts with pyridines [26].

In comparing the atomic distances found in the solid state structures of complexes **1**–**3**, it is evident in progressing down Group 15, the bond lengths become more elongated to compensate for the larger atomic radii. Except for the E–C bond length, a similar trend can be seen in the complex **4**. The E–Cl(1)–Cl(2) bond distances in **1**–**4** are unsymmetrical, with E–Cl(2) elongated in comparison to E–Cl(1). For **1**–**3** it is evident that as the size of E increases the difference in the E–C, E–N bond lengths is reduced.

Further details on the nitrogen interaction in compounds **1**–**3** is presented in Table 2 which compares the angles within the N–C–C–E ring (E = Hg [27], P, As, Sb). Examining the P, As and Sb analogues reveals that they are within 4° of each other. In the mercury compound, where there is no internal dative bonds, the angle at C–C–Hg is significantly more open, giving a distorted tetrahedral angle of 117°. Coinciding with the distorted geometry is the near linear C–Hg–C bond

length, indicating that the reduction in bond angle in **1**, **2** and **3** cannot be solely due to the bulk of the $SiMe_3$, and that a N···E bonding interaction is present. This is consistent with the persistence of such an interaction in the less sterically congested complex $[r'SbCl_2]_2$ (**4**), but not necessarily in the corresponding phosphorus complex, which unfortunately we have been unable to isolate.

2.3. Solution studies

In compounds **2** and **3** the ^1H and ^{13}C are unremarkable, except for a significant downfield shift (32.9 → 50.2/65.10 ppm (As, Sb)) for the carbon adjacent to the trimethylsilyl groups, relative to R′H. This reflects the negative charge on C induced by replacement of the proton with E. A similar downfield shift is seen in compound **1**, (32.9 → 52.0 ppm), but unlike **2** and **3**, in the ^1H-NMR there are two signals for the inequivalent $SiMe_3$ groups. It is likely that in solution the As–N, Sb–N bond breaks and the time averaged occupation of the $SiMe_3$ groups results in a singlet, whereas the P–N remains intact showing the inequivalent groups as two singlets. ^{31}P-NMR revealed a sharp singlet at 175.1 ppm which is in the region comparable to (2,4,6-$^tBu_3C_6H_2$)PCl_2 [28], 155 ppm, and $[(Me_3Si)_3C]PCl_2$ [29], 233 ppm.

2.4. Theoretical studies

The electronic origin of these short intramolecular N···E dative bonds has been investigated using approximate density functional theory, focusing on the phosphorus compound, **1**. Calculations were performed on the complete molecule, and also a model compound, **1′**, in which the trimethylsilyl groups have been replaced by hydrogens. This comparison of the two systems allows the separation, at least approximately, of the intrinsic electronic stability of the N(1)–P(1) bond from the steric effects connected with the bulky trimethylsilyl group. Optimised geometries for both **1** and **1′** are shown in Fig. 2. In **1**, the P(1)–C(1)–C(2)–N(1) atoms are almost coplanar (torsion angle 4.8°), with a relatively short P–N separation of 2.38 Å and an elongated axial P(1)–Cl(1) bond, consistent with a significant interaction between the nitrogen-based lone pair and the P(1)–Cl(1) σ^* orbital. Despite the fact that the calculated N(1)–P(1) and P(1)–Cl(1) bonds are significantly longer and shorter, respectively, than those in the crystal structure, the calculations reproduce the key feature of interest, the presence of a significant N(1)–P(1) interaction. The strength of the interaction is clearly somewhat underestimated in the current calculations, but this does not prevent drawing some qualitative conclusions concerning its electronic origin.

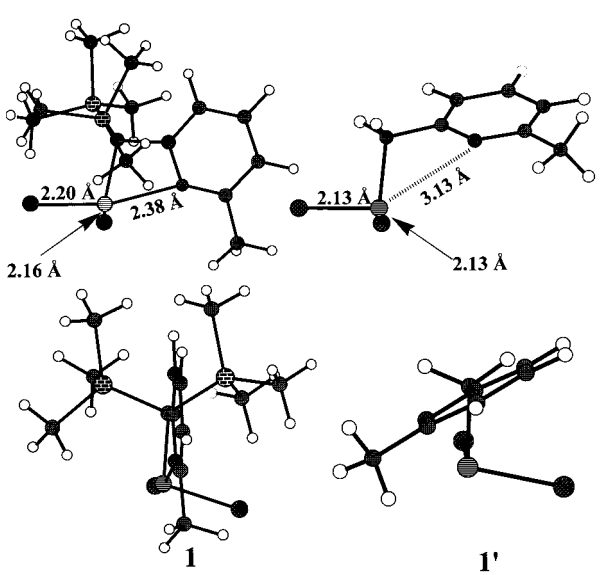

Fig. 2. Geometries for **1** and **1′**.

In marked contrast to compound **1**, no evidence of similar N(1)–P(1) interactions emerges in **1′**, where the trimethylsilyl groups have been removed. In the optimised structure, the pyridine ring is rotated by ca. 60° out of the plane defined by P(1)–C(1)–C(2), and the P(1)–C(1)–C(2) angle itself expands to 117.1° (compared to 95.6° in **1**). The net result is a large increase in the N(1)–P(1) distance (3.13 Å) and an equilibration of the two P(1)–Cl bond lengths. The fact that the simplest model compound, **1′** shows no evidence of a short N(1)–P(1) contact suggests that the intrinsic strength of the N–P bond is not the origin of the unusual structures observed in these systems. The influence of the trisilylmethyl groups in **1** can be separated, at least conceptually, into two parts, both related to their steric bulk. The Si–C(1)–Si angle is significantly larger than H–C(1)–H in **1′**, a change that will in turn reduce the P(1)–C(1)–C(2) angle (a phenomenon known as the Ingold effect), and therefore the N(1)–P(1) separation. The influence of the Ingold effect was investigated by reoptimising the structure of **1′** with the H–C(1)–H angle frozen at 114.5°, the optimised value of Si–C(1)–Si in **1**. This structural distortion (and even larger angles to 120°) was found to have a negligible effect on the remainder of the structure, suggesting that the Ingold effect is not the driving force for the short N(1)–P(1) bond. The second major effect of the bulky trimethylsilyl groups is to control the conformation of the pyridine ring, which lies in a groove defined by the six methyl groups (see Fig. 2). Any rotation about the C(1)–C(2) bond (as observed in **1′**) is opposed by non-bonded repulsions between pyridine and the methyl groups, effectively anchoring the ring in the P(1)–C(1)–C(2) plane and forcing the nitrogen-based lone pair in the ideal position to interact with the

phosphorus centre. Consistent with this hypothesis, if the pyridine ring in **1′** is constrained to lie in the P(1)–C(1)–C(2) plane, the P–N bond length is reduced to 2.68 Å.

3. Conclusions

We have shown that the reaction of R′Li (where R′ = 6-Me-2-Pyr($SiMe_3$)$_2$C$^-$) with ECl_3 (E = P, As, Sb) results in the crystallisation of the corresponding R′ECl_2 species for all three Group 15 adducts. In all complexes the geometry about the E centre is a distorted trigonal bipyramidal, and a short intramolecular dative bond between the pyridyl nitrogen and the E centre is present in all cases. When the less bulky ligand r′ is employed under the same conditions, the reduction in steric bulk leads to less protection at the antimony centre, and a dimeric complex is formed. We have also shown that approximate density functional theory successfully models the unusual structural features of compound **1**, although the magnitude of the effect is somewhat underestimated. The origin of the effect is traced to the steric bulk of the trimethylsilyl groups, which force the pyridine ring to lie in the plane defined by the Cl(1)–P(1)–C(1) triad. If these steric constraints are removed, the intrinsic strength of the bond is insufficient to prevent rotation of the pyridine ring.

4. Experimental

4.1. General procedures

All operations were performed under dry argon on a vacuum line using standard Schlenk techniques or in an Argon atmosphere dry box. The solvents used (hexane, diethyl ether, THF) were dried over sodium wire prior to distillation over a Na–K alloy and stored over a sodium mirror under argon prior to their use. ^{1}H, ^{13}C, ^{31}P were recorded on a Bruker DRX400 or Varian AM300 spectrometer. Chemical shifts were referenced relative to benzene-d_6, while ^{31}P was referenced relative to 85% phosphoric acid. R′ is labelled from the carbon bearing the trimethyl substituents as **1**, working anticlockwise around the ring, to finish with the methyl substituent being labelled as **7**. PCl_3, $AsCl_3$ were distilled prior to use and stored under argon. ^{n}BuLi was purchased from Aldrich as a 1.6 M solution in hexane and used without any further purification. Elemental analysis was performed by CMAS Pty. Ltd. Due to thermal instability there was no microanalysis on compound **1**.

4.1.1. [{6-methyl-2-bis(trimethylsilyl)methylpyridine}-phosphorus dichloride] [R′PCl_2] (1)

^{n}BuLi (3.5 ml, 5.6 mmol) was added slowly to a solution of 6-methyl-2-bis(trimethylsilyl)methylpyridine (1.29 g, 5.1 mmol) in Et_2O (30 ml) at 0°C. The orange solution was stirred for 30 min at room temperature. This solution was then cooled to −78°C and added over 10 min to a solution of PCl_3 (0.45 ml, 5.2 mmol) in Et_2O (30 ml) at −78°C. The dark orange solution was stirred, and allowed to warm slowly to ambient temperature over 6 h. Volatiles were removed in vacuo and the resulting orange powder extracted into hexane. Filtration, concentration and cooling to −30°C yielded large orange plates. Typical yield: 1.16 g, 66%. M.p. 65–66°C (decomposition).

^{1}H-NMR (300 MHz, C_6D_6, 25°C): δ 0.33 (9H, s, $SiMe_3$), 0.34 (9H, s, $SiMe_3$), 2.19 (3H, s, CH_3), 6.26 (1H, m, H^3), 6.89 (1H, m, H^5), 6.95 (1H, m, H^4). ^{13}C-NMR (75.0 MHz, C_6D_6, 25°C): δ 2.31 ($SiMe_3$), 2.47 ($SiMe_3$), 22.8 (C^7), 52.0 (C^1), 119.1 (C^5), 120.3 (C^3), 136.1 (C^4), 156.9 (C^6), 163.9 (C^2). ^{31}P-NMR (162 MHz, C_6D_6, 25°C): δ 175.1.

4.1.2. [{6-methyl-2-bis(trimethylsilyl)methylpyridine}-arsenic dichloride] [R′$AsCl_2$] (2)

^{n}BuLi (12.5 ml, 19.1 mmol) was added slowly to a solution of 6-methyl-2-bis(trimethylsilyl)methylpyridine (4.63 g, 18.4 mmol) in Et_2O (100 ml) at 0°C. The orange solution was stirred for 45 min at room temperature. This solution was then cooled to −78°C and added over 10 min to a solution of $AsCl_3$ (1.60 ml, 19.1 mmol) in Et_2O (70 ml) at −78°C. The yellow solution was stirred, and allowed to warm slowly to ambient temperature over 6 h. Volatiles were removed in vacuo and the resulting yellow powder extracted into hexane. Filtration, concentration and cooling to −30°C yielded yellow needles. Typical yield: 1.31g, 68%. M.p. 145–148°C.

^{1}H-NMR (300 MHz, C_6D_6, 25°C): δ 0.34 (18H, s, $SiMe_3$), 2.05 (3H, s, CH_3), 6.29 (1H, m, H^3), 6.60 (1H, m, H^5), 6.93 (1H, m, H^4). ^{13}C-NMR (75.0 MHz, C_6D_6, 25°C): δ 1.9 ($SiMe_3$), 20.5 (C^7), 50.2 (C^1), 118.4 (C^5), 120.0 (C^3), 137.5 (C^4), 155.1 (C^6), 162.9 (C^2). Elemental analysis: Required: C, 39.39; H, 6.10; N, 3.53. Found: C, 39.62; H, 6.12; N, 3.71%.

4.1.3. [{6-methyl-2-bis(trimethylsilyl)methylpyridine}-antimony dichloride] [R′$SbCl_2$] (3)

^{n}BuLi (4.6 ml, 7.1 mmol) was added slowly to a solution of 6-methyl-2-bis(trimethylsilyl)methylpyridine (1.75 g, 7.0 mmol) in Et_2O (30 ml) at 0°C. The orange solution was stirred for 45 min at room temperature. This solution was then cooled to −78°C and added over 10 min to a solution of $SbCl_3$ (1.6 g, 7.1 mmol) in Et_2O (30 ml) at −78°C. The yellow solution was stirred, and allowed to warm slowly to ambient temper-

ature over 6 h was stirred. Volatiles were removed in vacuo and the resulting white powder extracted into hexane. Filtration, concentration and cooling to −30°C yielded colourless prisms. Typical yield: 2.30 g, 74%. M.p. 127°C

^{1}H-NMR (300 MHz, C_6D_6, 25°C): δ 0.32 (18H, s, $SiMe_3$), 1.94 (3H, s, CH_3), 6.23 (1H, m, H^3), 6.57 (1H, m, H^5), 6.91 (1H, m, H^4); ^{13}C NMR (75.0 MHz, C_6D_6, 25°C): δ 2.3 ($SiMe_3$), 20.5 (C^7), 65.12 (C^1), 119.7 (C^5), 122.6 (C^3), 139.0 (C^4), 154.8 (C^6), 163.5 (C^2). Elemental analysis: Required: C, 35.23; H, 5.46; N, 3.16. Found: C, 34.82; H, 5.56; N, 3.66%.

4.1.4. [{6-methyl-2-(trimethylsilyl)methylpyridine}-antimony dichloride] [r′$SbCl_2$]$_2$ (**4**)

^{n}BuLi (1.88 ml, 3.0 mmol) was added slowly to a solution of 6-methyl-2-(trimethylsilyl)methylpyridine (0.5 g, 2.8 mmol) in THF (30 ml) at 0°C. The orange solution was stirred for 45 min at room temperature. This solution was then cooled at −78°C and added over 10 min to a solution of $SbCl_3$ (0.63 g, 2.75 mmol) in THF (30 ml) at −78°C. The yellow solution was stirred, and allowed to warm slowly to ambient temperature over 6 h. Volatiles were removed in vacuo and the resulting white powder extracted into hexane. Filtration, concentration and cooling to −30°C yielded colourless prisms.

Typical yield: 0.6 g 58%. M.p. 89–90°C, 140°C (decomposition). ^{1}H-NMR (300 MHz, C_6D_6, 25°C): δ 0.10 (9H, s, $SiMe_3$), 2.01 (3H, s, CH_3), 6.28 (2H, m, H^3, H^5), 6.92 (1H, m, H^4); ^{13}C-NMR (75.0 MHz, C_6D_6, 25°C): δ −0.3 ($SiMe_3$), 21.82 (C^7), 51.1 (C^1), 119.7 (C^5), 121.5 (C^3), 138.4 (C^4), 147.3 (C^6), 162.9 (C^2). Elemental analysis: Required: C, 32.38; H, 4.35; N, 3.78. Found: .C, 31.96; H, 4.68; 4.19%.

4.2. Computational details

All calculations described in this paper were performed using the Amsterdam Density Functional (ADF99) program [30,31], developed by Baerends and co-workers. A double-ζ Slater-type basis set, extended with a single polarisation function, was used to describe all atoms in the molecule. Electrons in orbitals up to and including 1s {C,N} and 2p {P,Cl}, were considered part of the core and treated in accordance with the frozen core approximation. The local density approximation was employed in all cases [32], along with the local exchange-correlation potential of Vosko, Wilk and Nusair [33] and gradient corrections to exchange and correlation proposed by Becke and Perdew [34,35]. Structures were optimised using the gradient algorithm of Versluis and Ziegler [36]. No symmetry restrictions were imposed.

4.3. Structure determinations

Unique room temperature single counter diffractometer data sets were measured ($2\theta_{max}$ as specified; 2θ–θ scan mode; T ca. 293 K; monochromatic Mo–K_α

Table 3
Crystallographic data

	1	**2**	**3**	**4**
Formula	$C_{13}H_{24}Si_2NPCl_2$	$C_{13}H_{24}Si_2NAsCl_2$	$C_{13}H_{24}Si_2NSbCl_2$	$C_{10}H_{16}Cl_2NSbSi$
Formula weight	354.41	396.34	443.2	370.99
Crystal system	Monoclinic	Monoclinic	Triclinic	Triclinic
Space group	$P2_1/n$	$P2_1/c$	$P\bar{1}$	$P\bar{1}$
a (Å)	8.729(6)	8.764(2)	13.600(6)	12.158(2)
b (Å)	13.06(1)	13.422(8)	8.900(2)	9.339(5)
c (Å)	16.16(1)	17.361(6)	8.522(2)	7.015(1)
α (°)	90.0	90.0	71.55(2)	103.95(3)
β (°)	99.02(6)	111.15	80.98(3)	101.75(1)
γ (°)	90.0	90.0	84.86(3)	95.57(3)
V (Å^3)	1819(2)	1905(1)	965.5(5)	101.75(1)
Z	4	4	2	1 (dimer)
F(000)	752	816	444	364
D_{calc} (g cm^{-3})	1.29	1.382	1.52	1.65
Dimensions	$0.4\times0.65\times0.1$	$0.45\times0.70\times0.12$	$0.40\times0.38\times0.08$	$0.10\times0.47\times0.22$
μ (cm^{-1})	5.6	21.8	18.2	22.5
A^* min, max	–	1.28, 2.31	1.15, 1.89	1.75, 1.96
2θ max (°)	50	55	55	60
Unique	3367	3942	4031	4250
μ_o ($I>3\sigma(I)$)	2392 [a]	2768	3337	3330
R	0.045	0.035	0.032	0.037
R_w	0.034	0.036	0.036	0.041

[a] $\mu_o(I>2\sigma(I))$.

radiation, $\lambda = 0.71073$ Å), yielding N independent reflections, N_o with $I > 3\sigma(I)$ being considered 'observed' and used in the full-matrix least squares refinements after absorption correction. Anisotropic thermal parameter forms were refined for the non-hydrogen atoms, $(x, y, z, U_{iso})_H$HH being included constrained at estimated values. Conventional residuals R, R_w (statistical weights) on $|F|$ are quoted at convergence. Neutral atom complex scattering factors were employed, computation using the XTAL 3.4 program system [37]. Pertinent results are given below and in the Fig. 1(a–b) and Tables 1–3, individual variations in procedure, difficulties, idiosyncrasies being noted below:

1. $(x, y, z, U_{iso})_H$HH were refined.
2. Hydrogen atoms were located in difference maps, but not refined.

Acknowledgements

We thank the Australian Research Council for financial support and Monash University for a Postgraduate Publication Award (BAR).

References

[1] P. Power, J. Chem. Soc. Dalton Trans. (1998) 2939.
[2] M. Yoshifuji, I. Shima, N. Inamoto, J. Am. Chem. Soc. 103 (1981) 4587.
[3] N. Tokitoh, Y. Arai, R. Okazaki, S. Nagase, Science 277 (1997) 78.
[4] T.R. van den Ancker, C.L. Raston, J. Organomet. Chem. 500 (1995) 289.
[5] C. Jones, L.M. Engelhardt, P.C. Junk, D.S. Hutchings, W.C. Patalinghug, C.L. Raston, A.H. White, Chem. Comm. (1991) 1560.
[6] P.C. Andrews, C.L. Raston, B.W. Skelton, V.-A. Tolhurst, A.H. White, Chem. Comm. (1998) 575.
[7] A.H. Cowley, N.C. Norman, M. Pakulski, J. Chem. Soc. Dalton Trans. (1985) 383.
[8] Search of the Cambridge crystal structure data base, 1/12/99.
[9] F. Carré, C. Chuit, R.J.P. Corriu, P. Monforte, C. Reyé, J. Declercq, A. Dubourg, Angew. Chem. Int. Ed. Engl. 32 (1993) 1430.
[10] J. Bezombes, F. Carré, C. Chuit, R.J.P. Corriu, A. Mehdi, C. Reyé, J. Organomet. Chem. 535 (1997) 81.
[11] W. Honeise, W. Schwarz, G. Heckmann, A. Schmidt, Z. Allorg. Allg. Chem. 533 (1986) 55.
[12] D.K. Kennepohl, A.A. Pinkerton, Y.F. Lee, R.G. Cavell, Inorg. Chem. 29 (1990) 5088.
[13] A. Bondi, J. Phys. Chem. 68 (1964) 441.
[14] H. Schumann, F.H. Gorlitz, M. Schaters, Acta Crystallogr. Sect. C 49 (1993) 688.
[15] B.N. Meyer, J.N. Ishley, A.V. Fratini, H.C. Knachel, Inorg. Chem. 19 (1980) 2324.
[16] M. Webster, S. Keats, J. Am. Chem. Soc. 4 (1971) 836.
[17] C.J. Carmalt, A.H. Cowley, R.D. Culp, R.A. Jones, S. Kamepalli, N.C. Norman, Inorg. Chem. 36 (1997) 2770.
[18] A. Brandl, H. Nöth, Chem. Ber. 121 (1988) 1321.
[19] S. Kamepalli, C.J. Carmalt, R.D. Culp, A.H. Cowley, R.A. Jones, Inorg. Chem. 35 (1996) 6179.
[20] J.-T. Ahlemann, H.W. Roesky, R. Murugavel, E. Parisini, M. Noltemeyer, H.-G. Schmidt, O. Müller, R. Herbst-Irmer, L.N. Markovski, Y.G. Shermolovich, Chem. Ber. 130 (1997) 1113.
[21] R.O. Day, J.M. Holmes, A.C. Sau, J.R. Devillers, R.R. Holmes, J.A. Deiters, J. Am. Chem. Soc. 104 (1982) 2127.
[22] D.A. Atwood, A.H. Cowley, J. Ruiz, Inorg. Chim. Acta. 198–200 (1992) 271.
[23] G. Ferguson, R.G. Goel, D.R. Ridley, J. Chem. Soc. Dalton Trans. (1975) 1288.
[24] A. Strube, G. Huttner, L. Zsolnai, J. Organomet. Chem. 399 (1990) 255.
[25] U. Patt-Stiebel, U. Müller, C. Ergezinger, B. Borgsen, K. Dehicke, Z. Anorg. Allg. Chem. 582 (1990) 30.
[26] C.L. Raston, G.L. Rowbottom, A.H. White, J. Chem. Soc. Dalton Trans. (1981) 1379.
[27] T.R. van den Ancker, C.L. Raston, unpublished results.
[28] A.H. Cowley, N.C. Norman, M. Pakuslki, in: A.P. Ginsberg (Ed.), Inorganic Synthesis, vol. 27, Wiley–Interscience, New York, 1990, pp. 235.
[29] K. Issleib, M. Schmidt, C. Wirkner, Z. Chem. 20 (1986) 153.
[30] E.J. Baerends, A. Bérces, C. Bo, P.M. Boerrigter, L. Cavallo, L. Deng, R.M. Dickson, D.E. Ellis, L. Fan, T.H. Fischer, C. Fonseca Guerra, S.J.A. van Gisbergen, J.A. Groeneveld, O.V. Gritsenko, F.E. Harris, P. van den Hoek, H. Jacobsen, G. van Kessel, F. Kootstra, E. van Lenthe, V.P. Osinga, P.H.T. Philipsen, D. Post, C.C. Pye, W. Ravenek, P. Ros, P.R.T. Schipper, G. Schreckenbach, J.G. Snijders, M. Sola, D. Swerhone, G. te Velde, P. Vernooijs, L. Versluis, O. Visser, E. van Wezenbeek, G. Wiesenekker, S.K. Wolff, T.K. Woo, T. Ziegler, ADF, 1999.
[31] C. Fonseca Guerra, J.G. Snijders, G. te Velde, E.J. Baerends, Theor. Chem. Acc. 99 (1998) 391.
[32] R.G. Parr, W. Yang, Density Functional Theory of Atoms and Molecules, Oxford University Press, New York, 1989.
[33] S.H. Vosko, L. Wilk, M. Nusair, Can. J. Phys. 58 (1980) 1200.
[34] A.D. Becke, Phys. Rev. Sect. A 38 (1988) 3098.
[35] J.P. Perdew, Phys. Rev. Sect. B 33 (1986) 8822.
[36] L. Versluis, T. Ziegler, J. Chem. Phys. 88 (1988) 322.
[37] S.R. Hall, G.S.D. King, J.M. Stewart (Eds.), The XTAL 3.4 Reference Manual, University of Western Australia, Lamb, Perth, 1985.